Spectrum Sensing in Full-Duplex Cognitive Radio Networks Under Hardware Imperfections

Alexandros-Apostolos A. Boulogeorgos, *Student Member, IEEE*, Haythem A. Bany Salameh, *Senior Member, IEEE*, and George K. Karagiannidis, *Fellow, IEEE*

***Abstract*—Direct-conversion radio transceivers can offer reprogrammable and low-cost hardware solutions for full-duplex (FD) cognitive radio networks (CRNs). However, they are susceptible to radio-frequency (RF) impairments, such as in-phase (I) and quadrature (Q) imbalance (IQI), which can significantly limit spectrum sensing capabilities. This paper is devoted to quantifying and evaluating the effects of IQI in single- and multichannel energy detectors operating in FD mode under both cooperative and noncooperative spectrum sensing scenarios. In this context, closed-form expressions are derived for the false alarm and detection probabilities in the general case, where partial self-interference suppression (SIS) and joint transmitter (TX) and receiver (RX) IQI are considered. Furthermore, simplified closed-form expressions for the special cases, where either the RF front end is ideal or the SIS technique is perfect, are also presented. The presented analytical results have been verified through extensive simulations and indicate that the IQI and partial SIS can significantly affect spectrum sensing accuracy in FD-based CRNs. Specifically, if ideal RF front end is assumed, spectrum sensing error can significantly increase, leading to a reduction in the CRN performance and a negative effect on the performance of primary (PR) networks. Hence, when designing spectrum sharing algorithms for FD-based CRNs, the hardware impairments should be considered to improve the CRN performance while minimizing the negative effects on PR users.**

***Index Terms*—Cognitive radio (CR), full-duplex (FD), hardware constraints, in-phase/quadrature (I/Q) imbalance, multichannel energy detectors (EDs), radio-frequency (RF) impairments, single-channel EDs, spectrum sensing.**

I. Introduction

THE rapid growth of wireless communications and the foreseen spectrum occupancy problems have inspired the evolution of the concept of cognitive radio (CR) [1]. As a result, CR has been recently adopted in several wireless communication standards, such as Long-Term Evolution [2], WiFi (IEEE 802.11), Zigbee (IEEE 802.15.4), and WiMAX (IEEE 802.16) [3]. In traditional CR scenarios, the transceivers operate in half-duplex (HD) mode (i.e., at a given time interval, they can either transmit or receive/sense but not both). However, the feasibility of enabling full-duplex (FD) CR communications (i.e., transmit and receive/sense simultaneously over the same frequency channel) has been recently demonstrated by combining traditional and novel self-interference suppression (SIS) techniques [4].

One essential functionality in the operation of CRs, whether they operate in HD or FD mode, is spectrum sensing (identifying temporarily vacant portions of spectrum). As a consequence, a great deal of effort was put in deriving optimal, suboptimal, ad hoc, and cooperative techniques, as well as analyzing their spectrum sensing capabilities [5]–[9]. Most of these studies assumed ideal radio frequency (RF) front end for the CR transceivers. However, practical CR devices suffer from hardware imperfections, such as low-noise amplifier nonlinearities [10], local oscillator phase noise [11], and in-phase (I) and quadrature (Q) imbalance (IQI) [12], [13]. Particularly, IQI corresponds to the amplitude and phase mismatch between the I and Q branches of a transceiver and ultimately leads to imperfect image rejection that incurs considerable performance degradation [13]–[15].

In the context of CRs, several studies have shown that these imperfections restrict the spectrum sensing capabilities of HD CR systems [10], [16]–[23]. More specifically, in [16], the negative effects of IQI on spectrum sensing were demonstrated, considering both cases of single- and multichannel secondary user (SU) direct-conversion receiver (RX). In [20], closed-form expressions for the detection and false alarm probabilities for the Neyman–Pearson detector were presented, considering the spectrum sensing problem in single-channel orthogonal frequency-division multiplexing CR system, under joint transmitter (TX) and RX IQI. On the other hand, the effects of transmit hardware imperfections in primary (PR) user (PU)–SU base station cooperative FD CR systems were investigated in [24], where the problem of interest was to find the achievable primary-cognitive rate region by studying the cognitive rate maximization problem. Nonetheless, in that work, the effects of transmit hardware impairments were approximated as a complex Gaussian process, whereas the effects of RX RF imperfections were neglected; as a result, the impact of RF impairments in the spectrum sensing capabilities of the CR devices was not taken into consideration. In summary, several communication protocols and mechanisms have been proposed for CR networks (CRNs). However, most of them did not consider the effects of

Manuscript received October 26, 2015; revised March 15, 2016 and May 2, 2016; accepted June 14, 2016. Date of publication June 21, 2016; date of current version March 10, 2017. The work of H. A. B. Salameh was supported by the European Union Humanities Education Revitalized via Mundus Experiences (HERMES) mobility fund under the framework of the Erasmus Mundus Action 2, Strand 1 Projects, which was carried out at the Aristotle University of Thessaloniki, Greece, where he was a visiting Research Professor. A limited subset of initial results was preliminarily presented at the IEEE WCNC'2016 International Workshop on Smart Spectrum (IWSS 2016), Qatar. The review of this paper was coordinated by Dr. L. Zhao.

A.-A. A. Boulogeorgos and G. K. Karagiannidis are with the Department of Electrical and Computer Engineering, Aristotle University of Thessaloniki, 541 24 Thessaloniki, Greece (e-mail: ampoulog@auth.gr; geokarag@auth.gr).

H. A. B. Salameh is with the Department of Telecommunications Engineering, Yarmouk University, Irbid 21163, Jordan (e-mail: haythem@yu.edu.jo).

Digital Object Identifier 10.1109/TVT.2016.2582790

hardware impairments, which can severely degrade the CRNs' performance.

To the best of the authors' knowledge, the detrimental effects of IQI and partial SIS in FD CRNs have not been addressed in the open technical literature. Motivated by this, as well as the recent developments in FD CR communications, we study the joint impact of the RF impairments and partial SIS on the CR device's spectrum sensing capabilities. Specifically, the contribution of this paper can be summarized as follows.

- Signal models that describe the joint effects of IQI and partial SIS are presented for single- and multichannel energy detectors (EDs).
- We derive an analytical framework to evaluate the false alarm and detection probabilities of both single- and multichannel EDs that are constrained by hardware imperfections for FD-based CR systems.
- Based on the derived expressions for the false alarm and detection probabilities, we compare the spectrum sensing capabilities of the I/Q imbalanced FD-based CRs with the ideal RF front-end FD CRs and the corresponding HD system.
- We extend the analysis in the case of cooperative sensing, where each SU has different IQI and SIS capability levels. Each SU independently senses each PR channel, estimates whether it is busy or idle, and reports its estimation to the other SUs. Then, each SU decides the availability of the sensed channel using the AND, the OR, or the MAJORITY rule to combine the SUs' estimations.
- Finally, to demonstrate the detrimental effects of IQI and partial SIS, several examples of false alarm/detection probabilities and receiver operation curves (ROCs) are demonstrated for different SIS and IQI levels.

The rest of this paper is organized as follows. The system and signal models for both single- and multichannel EDs, when the transceivers suffer from IQI and partial SIS, are presented in Section II. The analytical framework for evaluating the false alarm and detection probabilities is provided in Section III, whereas in Section IV, we extend the analysis in the case of cooperative sensing. Numerical and simulation results that verify the analysis and illustrate the detrimental effects of IQI and partial SIS are presented in Section V. Finally, Section VI concludes this paper by summarizing its main contribution.

Notations: Unless otherwise stated, $\Re\{x\}$ and $\Im\{x\}$ represent the real and imaginary parts of x, respectively. The operators $E[\cdot]$ and $|\cdot|$ denote the statistical expectation and the absolute value, respectively, whereas the operators $\lceil x \rceil$ and $\text{card}(\mathcal{A})$ return the smallest integer greater than or equal to x and the cardinality of the set $\mathcal{A}$. Furthermore, $Q(x) = (1/\sqrt{2\pi}) \int_x^\infty e^{-t^2/2} dt$ stands for the Gaussian Q-function, whereas $\gamma(a, x)$ and $\Gamma(\cdot)$ are the lower incomplete Gamma function and the Gamma function, respectively, which are defined as [25, Eq. (8.350/1)] $\gamma(a, x) = \int_0^x e^{-t} t^{a-1} dt$ and [25, Eq. (8.310/1)] $\Gamma(x) = \int_0^\infty e^{-t} t^{a-1} dt$.

II. System and Signal Model

As demonstrated in Fig. 1, we consider a CRN that consists of several PUs, and the CR devices operate in FD mode. Each

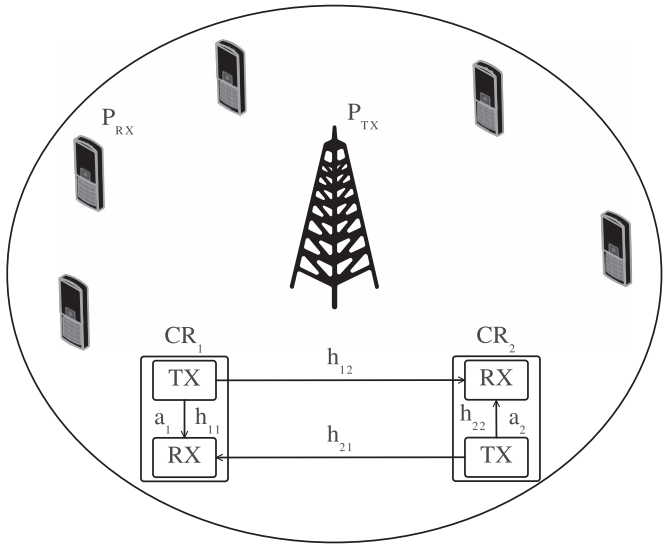

Fig. 1. SU link that opportunistically accesses the spectrum of a PR network.

SU CR device is considered to be a low-cost transceiver that suffers from joint TX/RX IQI. Furthermore, it is assumed that each SU i has partial SIS capability, which is measured by the degree of SIS ($a_i \in [0, 1]$). Note that if $a_i = 0$, the SU has complete SIS capability. We assume that the interference between SU links is resolved by implementing an appropriate multiple-access scheme (see, for example, [26] and [27]). Moreover, for both scenarios of single- and multichannel EDs, for simplicity and without any loss of generality, we ignore the path loss between the SU's TX and its RX at the same node, i.e., $h_{ii} = 1$. The channel gain between the TX i and the RX j at distance d_{ij} is $h_{ij} = C d_{i,j}^n$, where C is a frequency-dependent constant, and n is the path loss exponent.

A. Single-Channel Energy Detector

Note that sensing only one particular frequency channel at a time is a rather limited scenario in general CR and spectrum sensing context [16]. However, for completeness, we analyze the impact of IQI and partial SIS on the spectrum sensing performance of a single-channel ED.

Two hypotheses of PU absent/present can be determined through the parameter $\theta \in \{0, 1\}$. For a given θ, the nth sample of the received baseband equivalent signal for the SU i in the case of single-channel EDs can be expressed as

$$y_i(n) = \theta x_i(n) + a_i s_i(n) + w_i \tag{1}$$

where $x_i(n)$, $s_i(n)$, and $w_i(n)$ are the nth sample of the I/Q imbalanced received PU signal by the ith SU, the I/Q imbalanced received signal due to the SU's own transmission before applying SIS, and the I/Q imbalanced noise, respectively, which are given by [28]

$$x_i(n) = K_{1,i}^r x_{\text{id},i}(n) + K_{2,i}^r x_{\text{id},i}^*(n) \tag{2}$$

$$s_i(n) = \xi_{1,i} s_{\text{id},i} + \xi_{2,i} s_{\text{id},i}^* \tag{3}$$

$$w_i(n) = K_{1,i}^r w_{\text{id},i}(n) + K_{2,i}^r w_{\text{id},i}^*(n) \tag{4}$$

where $x_{\text{id},i}(n)$, $s_{\text{id},i}(n)$, and $w_{\text{id},i}(n)$ are the circularly symmetric complex white Gaussian (CSCWG) processes that

model the received PU signal, the received signal due to the SU's own transmission before applying SIS, and the received noise, when ideal RF front end is considered, respectively. The parameters $\xi_{1,i}$ and $\xi_{2,i}$ model the joint effect of TX/RX IQI and can be obtained as

$$\xi_{1,i} = K^r_{1,i}K^t_{1,i} + K^r_{2,i}\left(K^t_{2,i}\right)^* \quad (5)$$

$$\xi_{2,i} = K^r_{1,i}K^t_{2,i} + \left(K^t_{1,i}\right)^* K^r_{2,i} \quad (6)$$

where $K^t_{1,i}$, $K^t_{2,i}$, and $K^r_{1,i}$, $K^r_{2,i}$ stand for the TX and RX IQI coefficients, which are given by

$$K^t_{1,i} = \frac{1+\epsilon^t_i e^{j\phi^t_i}}{2}, \quad K^t_{2,i} = \frac{1-\epsilon^t_i e^{-j\phi^t_i}}{2} \quad (7)$$

$$K^r_{1,i} = \frac{1+\epsilon^r_i e^{-j\phi^r_i}}{2}, \quad K^r_{2,i} = \frac{1-\epsilon^r_i e^{j\phi^r_i}}{2} \quad (8)$$

with $\epsilon^{t/r}_i$ and $\phi^{t/r}_i$ denoting the amplitude and the phase imbalance at the TX/RX. Note that the IQI coefficients are connected through the following relation:

$$K^{\frac{t}{r}}_{1,i} = 1 - \left(K^{\frac{t}{r}}_{2,i}\right)^*. \quad (9)$$

Let IRR be the image rejection ratio, which is given by

$$\mathrm{IRR}^{\frac{t}{r}}_i = \frac{\left|K^{\frac{t}{r}}_{1,i}\right|^2}{\left|K^{\frac{t}{r}}_{2,i}\right|^2}. \quad (10)$$

Note that, for practical transceivers, IRR is in the range of [20, 40 dB] [15], [30]–[38].

By substituting (9) into (5) and (6) and after some algebraic manipulations, we show that

$$\xi_{1,i} = 1 - \xi^*_{2,i}. \quad (11)$$

It is important to note that, according to (1)–(4), the received signal at the ith SU, i.e., y_i, is interfered not only by the transmitted signal $s_{\mathrm{id},i}$ but also by the signals $s^*_{\mathrm{id},i}$ and $x^*_{\mathrm{id},i}$, due to the effects of IQI. Moreover, based on the received signal model in (1), the sensing channel is either vacant with only channel noise or occupied by a PU signal together with the channel noise.

B. Multichannel Energy Detector

In the case of a multichannel ED, we assume that $2K$ RF channels, which are by denoted by

$$S_K = \{-K, \ldots, -1, 1, \ldots, K\} \quad (12)$$

are downconverted to baseband using the wideband direct-conversion principle. This scenario was also considered in [16], where the sensitivity of wideband energy detection in HD CR systems was illustrated.

The baseband equivalent received signal model for an arbitrary channel $k \in S_K$ at the ith SU is given by

$$\begin{aligned} y_{i,k}(n) = {} & \theta_k K^r_{1,i} x_{i,k}(n) + \theta_{-k} K^r_{2,i} x^*_{i,-k}(n) \\ & + \tilde{\theta}_k a_i \xi_{1,i} s_{i,k}(n) + \tilde{\theta}_{-k} a_i \xi_{2,i} s^*_{i,-k}(n) \\ & + K^r_{1,i} w_{i,k}(n) + K^r_{2,i} w^*_{i,-k}(n) \end{aligned} \quad (13)$$

where $x_{i,k}(n)$, $s_{i,k}(n)$, and $w_{i,k}(n)$ are zero-mean CSCWG processes with variances $\sigma^2_{x_{i,k}}$, $\sigma^2_{s_{i,k}}$, and $\sigma^2_{w_{i,k}}$, respectively, which represent the ideal received PU signal, the ideal received signal due to the SU's own transmission before applying SIS, and the received noise over channel k sampled at time instant n. The parameters $\theta_k \in \{0, 1\}$ and $\tilde{\theta}_k \in \{0, 1\}$ indicate the existence of a PU signal and a transmitted signal at channel k.

From (13), it is evident that the received signal at the arbitrary channel k at the ith SU, i.e., $y_{i,k}$, may be interfered not only by the transmitted signal at the channel k, i.e., $s_{i,k}$, but also by the transmitted signal at channel $-k$, i.e., $s^*_{i,-k}$, due to the joint effects of IQI and partial SIS, as well as by the received signal at channel $-k$, i.e., $x^*_{i,-k}$, due to the effects of IQI. The levels of interference depend on the levels of IQI and the degree of SIS, as well as the existence of PU and SU activities at channels k and $-k$.

III. False Alarm and Detection Probabilities

Here, we present closed-form expressions to evaluate the false alarm and detection probabilities of hardware-constrained EDs.

A. Single-Channel Energy Detector

In the case of the single-channel ED, we assume that the SU employs the classical ED, where the test statistics is evaluated according to [22] as

$$T_i = \frac{1}{N_s}\sum_{n=0}^{N_s-1} |y_i(n)|^2. \quad (14)$$

In (14), N_s is the number of complex samples used for spectrum sensing. This test statistics is compared against a given threshold γ to decide whether the channel is busy or idle, i.e., if $T_i < \gamma$, the ED decides that the channel is idle; otherwise, it is busy.

In the propositions and special cases that follow, we evaluate the cumulative distribution function (cdf) of the test statistics for the general case, where the CR devices suffer from the joint effects of TX/RX IQI and the SIS is partial. We also consider the special cases of ideal TX and RX RF front ends and perfect SIS.

Proposition 1: The distribution of the energy test statistics conditional to θ, when the SU has partial SIS and suffers from IQI, for a sufficiently large number of samples (N_s) can be well approximated by a Gaussian distribution with a cdf

$$F(\gamma|\theta) = 1 - Q\left(\frac{\gamma - \mu_\theta}{\sqrt{\sigma^2_\theta}}\right) \quad (15)$$

where μ_θ and σ^2_θ stand for the mean and the variance of the test statistics and are given by

$$\begin{aligned} \mu_\theta = {} & \left(\left|K^r_{1,i}\right|^2 + \left|K^r_{2,i}\right|^2\right)\left(\theta\sigma^2_{x_{\mathrm{id}}} + \sigma^2_{w_{\mathrm{id}}}\right) \\ & + a_i^2\left(|\xi_{1,i}|^2 + |\xi_{2,i}|^2\right)\sigma^2_{s,\mathrm{id}} \end{aligned} \quad (16)$$

$$\begin{aligned} \sigma^2_\theta = {} & \frac{1}{N_s}\Big(2\theta k_r \sigma^4_{x_{\mathrm{id},i}} + 2a_i^4 k_{t,r}\sigma^4_{s_{\mathrm{id},i}} + 2k_r\sigma^4_{w_{\mathrm{id},i}} + \theta k_{xw}\sigma^2_{x_{\mathrm{id}}}\sigma^2_{w_{\mathrm{id}}} \\ & + k_{xsw}\left(\theta\sigma^2_{x_{\mathrm{id}}} + \sigma^2_{w_{\mathrm{id}}}\right)a_i^2\sigma^2_{s_{\mathrm{id}}} - \mu^2_\theta\Big) \end{aligned} \quad (17)$$

where

$$k_r = \left|K_{1,i}^r\right|^4 + \left|K_{2,i}^r\right|^4 + 6\left|K_{1,i}^r\right|^2\left|K_{2,i}^r\right|^2 + 2\Re\left\{K_{1,i}^r\right\}^2\Im\left\{K_{1,i}^r\right\}^2 + 2\Re\left\{K_{2,i}^r\right\}^2\Im\left\{K_{2,i}^r\right\}^2 \tag{18}$$

$$k_{tr} = \left|\xi_{1,i}^r\right|^4 + \left|\xi_{2,i}^r\right|^4 + 6\left|\xi_{1,i}^r\right|^2\left|\xi_{2,i}^r\right|^2 + 2\Re\left\{\xi_{1,i}^r\right\}^2\Im\left\{\xi_{1,i}^r\right\}^2 + 2\Re\left\{\xi_{2,i}^r\right\}^2\Im\left\{\xi_{2,i}^r\right\}^2 \tag{19}$$

$$k_{xw} = \left(\left(2\Re\left\{K_{1,i}^r\right\} - 1\right)^2 + 4\Im\left\{K_{1,i}^r\right\}^2\right)^2 + 2\left(\left|K_{1,i}^r\right|^2 + \left|K_{2,i}^r\right|^2\right)^2 + 1 \tag{20}$$

$$k_{xsw} = \left(\left(2\Re\left\{K_{1,i}^r\right\} - 1\right)^2 + 4\Im\left\{K_{1,i}^r\right\}^2\right) \times \left(\left(2\Re\{\xi_{1,i}\} - 1\right)^2 + 4\Im\{\xi_{1,i}\}^2\right) + 2\left(\left|K_{1,i}^r\right|^2 + \left|K_{2,i}^r\right|^2\right)\left(|\xi_{1,i}|^2 + |\xi_{2,i}|^2\right) + 1. \tag{21}$$

Proof: See Appendix A. ■

Note that the exact distribution of the test statistics is rather complicated because of the dependence between the random variables ($\Re\{y_i\}$ and $\Im\{y_i\}$), due to the effects of IQI.

Now using the derived distribution for the test statistics, the false alarm and detection probabilities, when the SU has partial SIS and suffers from IQI, can be computed as

$$P_{\rm fa} = P_r(T > \gamma|\theta = 0) = Q\left(\frac{\gamma - \mu_0}{\sqrt{\sigma_0^2}}\right) \tag{22}$$

$$P_d = P_r(T > \gamma|\theta = 1) = Q\left(\frac{\gamma - \mu_1}{\sqrt{\sigma_1^2}}\right). \tag{23}$$

For a target false alarm probability $\tilde{P}_{\rm fa}$, the energy threshold can be evaluated using (22), which yields

$$\tilde{\gamma} = \sqrt{\sigma_0^2}Q^{-1}(\tilde{P}_{\rm fa}) + \mu_0 \tag{24}$$

whereas in this case, the detection probability, based on (23), is given by

$$\tilde{P}_d = Q\left(\frac{\sqrt{\sigma_0^2}Q^{-1}(\tilde{P}_{\rm fa}) + \mu_0 - \mu_1}{\sqrt{\sigma_1^2}}\right). \tag{25}$$

Special Case 1: In the case of partial SIS and ideal TX/RX RF front end, $K_{1,i}^t = K_{1,i}^r = 1$, $K_{2,i}^t = K_{2,i}^r = 0$, and, consequently, $\xi_{1,i} = 1$ and $\xi_{2,i} = 0$. Hence, based on (18)–(21), $k_r = k_{tr} = 1$, and $k_{xw} = k_{xsw} = 4$. Substituting these values into (16) and (17) and after some algebraic manipulations, we see that the mean and the variance of the SU received signal are, respectively, given by

$$\mu_\theta^2 = \theta\sigma_{x_{\rm id}}^2 + a_i^2\sigma_{s,{\rm id}}^2 + \sigma_{w_{\rm id}}^2, \qquad \sigma_\theta^2 = \frac{1}{N_s}\mu_\theta^2. \tag{26}$$

Special Case 2: In the case of perfect SIS and ideal TX/RX SU RF front ends, $K_{1,i}^t = K_{1,i}^r = \xi_{1,i} = 1$, $K_{2,i}^t = K_{2,i}^r = \xi_{2,i} = 0$, and $a_i = 0$. Substituting these values into (16) and (17), we prove that the mean and the variance of the SU received signal are, respectively, given by

$$\mu_\theta^2 = \theta\sigma_{x_{\rm id}}^2 + \sigma_{w_{\rm id}}^2 \qquad \sigma_\theta^2 = \frac{\mu_\theta^2}{N_s}. \tag{27}$$

Note that (27) coincides with [16, eq. (3)], which refers to an ideal RF front-end HD CR system. In other words, in the case of ideal RF front-end transceivers, regardless of whether the system operates in HD or FD mode with perfect SIS, the EDs achieve the same spectrum sensing capabilities.

Special Case 3: In the case of perfect SIS ($a_i = 0$) and joint TX/RX IQI, the mean and the variance of the SU received signal are, respectively, given by

$$\mu_\theta^2 = \left(\left|K_{1,i}^r\right|^2 + \left|K_{2,i}^r\right|^2\right)\left(\theta\sigma_{x_{\rm id}}^2 + \sigma_{w_{\rm id}}^2\right) \tag{28}$$

$$\sigma_\theta^2 = \frac{2\theta k_r\sigma_{x_{{\rm id},i}}^4 + 2k_r\sigma_{w_{{\rm id},i}}^4 + \theta k_{xw}\sigma_{x_{\rm id}}^2\sigma_{w_{\rm id}}^2 - \mu_\theta^2}{N_s}. \tag{29}$$

Proposition 2: In the case of ideal RF front end and partial SIS, the test statistics conditional to θ follows chi-square distribution with $2N_s$ degrees of freedom and a cdf given by

$$F(x|\theta) = \frac{\gamma\left(N_s, \frac{N_s x}{2\sigma_{y_{i|\theta}}^2}\right)}{\Gamma(N_s)} \tag{30}$$

where $\sigma_{y_{i|\theta}}^2$ is the variance of y_i obtained by

$$\sigma_{y_{i|\theta}}^2 = E\left[|y_{i|\theta}|^2\right] = \theta\sigma_{x_{\rm id}}^2 + a_i^2\sigma_{s_{\rm id}}^2 + \sigma_{w_{\rm id}}^2. \tag{31}$$

Proof: See Appendix B. ■

B. Multichannel Energy Detector

In the case of the multichannel ED, we assume that each SU employs the classical wideband ED, which calculates the test statistics at each channel k according to

$$T_{i,k} = \frac{1}{N_s}\sum_{n=0}^{N_s-1}\left|y_{i,k}(n)\right|^2. \tag{32}$$

Note that $T_{i,k}$ is compared against a threshold (γ) to decide whether the channel is busy or idle.

In the proposition that follows, we evaluate the cdf of the test statistics for the general case, where the CR devices suffer from the joint effects of TX/RX IQI and the SIS is partial.

Proposition 3: The distribution of the energy test statistics conditional to $\Theta = \{\theta_{-k}, \theta_k, \tilde{\theta}_{-k}, \tilde{\theta}_{-k}\}$, when the SU has partial SIS and suffers from IQI, for a sufficiently large number of samples (N_s), is Gaussian with a cdf

$$F(\gamma|\Theta) = 1 - Q\left(\frac{\gamma - \mu_\Theta}{\sqrt{\sigma_\Theta^2}}\right) \tag{33}$$

where μ_Θ and σ^2_Θ denote the mean and the variance of the test statistics, respectively, which are obtained as (34) and (35), shown at the bottom of the page. Note that α, β, δ, and ζ in (35) are as follows:

$$\alpha = \Re\left\{K^r_{1,i}\right\}\Re\left\{K^r_{2,i}\right\} + \Im\left\{K^r_{1,i}\right\}\Im\left\{K^r_{2,i}\right\} \quad (36)$$

$$\beta = \Re\left\{K^r_{1,i}\right\}\Im\left\{K^r_{2,i}\right\} + \Im\left\{K^r_{1,i}\right\}\Re\left\{K^r_{2,i}\right\} \quad (37)$$

$$\delta = \Re\{\xi_{1,i}\}\Re\{\xi_{2,i}\} + \Im\{\xi_{1,i}\}\Im\{\xi_{2,i}\} \quad (38)$$

$$\zeta = \Re\{\xi_{1,i}\}\Im\{\xi_{2,i}\} + \Im\{\xi_{1,i}\}\Re\{\xi_{2,i}\}. \quad (39)$$

Proof: See Appendix C. ■

Using the derived expressions for the energy test statistics distribution, the condition to Θ false alarm and detection probabilities, when the SU has partial SIS and suffers from IQI, can be derived by

$$P_{\rm fa}\left(\Theta = \{\theta_{-k}, \theta_k = 0, \tilde{\theta}_{-k}, \tilde{\theta}_k\}\right) = Q\left(\frac{\gamma - \mu_\Theta}{\sqrt{\sigma^2_\Theta}}\right) \quad (40)$$

$$P_d\left(\Theta = \{\theta_{-k}, \theta_k = 1, \tilde{\theta}_{-k}, \tilde{\theta}_k\}\right) = Q\left(\frac{\gamma - \mu_\Theta}{\sqrt{\sigma^2_\Theta}}\right). \quad (41)$$

Moreover, by considering that the PU existence parameter at image channel θ_{-k} and the SU existence parameters at channels $-k$ and k are Bernoulli distributed for any arbitrary channels (with success parameters p_{-k}, $\tilde{p}_{-k}$, and $\tilde{p}_k$, respectively), the false alarm and detection probabilities can be expressed as

$$\begin{aligned} P_{\mathcal{FA}} = & \sum_{\Theta\in\{\theta_{-k},\theta_k=0,\tilde{\theta}_{-k},\tilde{\theta}_k\}} (\theta_{-k}p_{-k} + (1-\theta_{-k})(1-p_{-k})) \\ & \times \left(\tilde{\theta}_{-k}\tilde{p}_{-k} + (1-\tilde{\theta}_{-k})(1-\tilde{p}_{-k})\right) \\ & \times \left(\tilde{\theta}_k\tilde{p}_k + (1-\tilde{\theta}_k)(1-\tilde{p}_k)\right) P_{\rm fa}(\Theta) \end{aligned} \quad (42)$$

$$\begin{aligned} P_{\mathcal{D}} = & \sum_{\Theta\in\{\theta_{-k},\theta_k=1,\tilde{\theta}_{-k},\tilde{\theta}_k\}} (\theta_{-k}p_{-k} + (1-\theta_{-k})(1-p_{-k})) \\ & \times \left(\tilde{\theta}_{-k}\tilde{p}_{-k} + (1-\tilde{\theta}_{-k})(1-\tilde{p}_{-k})\right) \\ & \times \left(\tilde{\theta}_k\tilde{p}_k + (1-\tilde{\theta}_k)(1-\tilde{p}_k)\right) P_d(\Theta). \end{aligned} \quad (43)$$

Note that $P_{\mathcal{FA}}$ and $P_{\mathcal{D}}$ are affected not only by the level of IQI and the SIS technique's capabilities but by the uncertainty of the PU signal over channels k and $-k$ and the uncertainty of the transmitted signals at k and $-k$ as well.

IV. Cooperative Sensing

As stated previously, the operation of a CRN should address an essential issue of identifying spectrum opportunities to enable an efficient spectrum utilization. Several studies have focused on this issue based on spectrum sensing in a cooperative or a noncooperative manner assuming ideal RF front end. Noncooperative sensing is easy to implement in practical settings, and its processing overhead is small. On the other hand, cooperative spectrum sensing can provide much better sensing accuracy, which might countermeasure the effects of IQI and partial SIS, at the expense of extra processing and control overhead [39], [40].

Here, we extend the analysis in Section III to investigate the performance of cooperative sensing under hardware impairments. Specifically, we consider that each one of the $N_{\rm su}$ SUs makes a binary decision on the PU activity, and the individual decisions are reported to the other SUs over a narrow-bandwidth error-free reporting channel, i.e., common control channels (CCCs) [27]. Note that the existence of CCC is a characteristic of many communication protocols designed for CRNs. We assume that the decision rule is the OR, the AND, or the MAJORITY, i.e., the presence of primary activity is decided if at least one SU, all, or the majority of the SUs individually decides that the sensing channel is busy.

In the propositions that follow, we evaluate the false alarm and detection probabilities of the CRNs for the case in which the OR, the MAJORITY, or the AND rule is used and the CR devices suffer from different levels of TX/RX IQI and the SIS.

Proposition 4: If the OR rule is employed, then the false alarm and detection probabilities can be expressed as

$$P_{C,\rm fa} = 1 - \prod_{i=1}^{N_{\rm su}} (1 - P_{{\rm fa},i}) \quad (44)$$

$$P_{C,d} = 1 - \prod_{i=1}^{N_{\rm su}} (1 - P_{d,i}) \quad (45)$$

$$\mu_\Theta = \theta_k \left|K^r_{1,i}\right|^2 \sigma^2_{x_{i,k}} + \theta_{-k}\left|K^r_{2,i}\right|^2 \sigma^2_{x_{i,-k}} + \tilde{\theta}_k a_i^2 |\xi_{1,i}|^2 \sigma^2_{s_{i,k}} + \tilde{\theta}_{-k} a_i^2 |\xi_{2,i}|^2 \sigma^2_{s_{i,-k}} + \left|K^r_{1,i}\right|^2 \sigma^2_{w_{i,k}} + \left|K^r_{2,i}\right|^2 \sigma^2_{w_{i,-k}} \quad (34)$$

$$\begin{aligned} \sigma^2_\Theta = \frac{1}{N_s} \Big(& 2\theta_k \left|K^r_{1,i}\right|^4 \sigma^4_{x_{i,k}} + 2\theta_{-k}\left|K^r_{2,i}\right|^4 \sigma^4_{x_{i,-k}} + 2\theta_k\theta_{-k}\left(\left|K^r_{1,i}\right|^2 \left|K^r_{2,i}\right|^2 + \alpha^2 + \beta^2\right) \sigma^2_{x_{i,k}} \sigma^2_{x_{i,-k}} \\ & + 2\tilde{\theta}_k a_i^4 \left|xi_{1,i}\right|^4 \sigma^4_{s_{i,k}} + 2\tilde{\theta}_{-k} a_i^4 |\xi_{2,i}|^4 \sigma^4_{s_{i,-k}} + 2\tilde{\theta}_k\tilde{\theta}_{-k} a_i^4 \left(|\xi_{1,i}|^2 |\xi_{2,i}|^2 + \delta^2 + \zeta^2\right) \sigma^2_{s_{i,k}} \sigma^2_{s_{i,-k}} \\ & + 2\left|K^r_{1,i}\right|^4 \sigma^4_{w_{i,k}} + 2\left|K^r_{2,i}\right|^4 \sigma^4_{w_{i,-k}} + 2\left(\left|K^r_{1,i}\right|^2 \left|K^r_{2,i}\right|^2 + \alpha^2 + \beta^2\right) \sigma^2_{w_{i,k}} \sigma^2_{w_{i,-k}} \\ & + 2a_i^2 \left(\theta_k \left|K^r_{1,i}\right|^2 \sigma^2_{x_{k,i}} + \theta_{-k}\left|K^r_{2,i}\right|^2 \sigma^2_{x_{-k,i}}\right) \left(\tilde{\theta}_k |\xi_{1,i}|^2 \sigma^2_{s_{k,i}} + \tilde{\theta}_{-k} |\xi_{2,i}|^2 \sigma^2_{s_{-k,i}}\right) \\ & + 2\left(\theta_k \left|K^r_{1,i}\right|^2 \sigma^2_{x_{k,i}} + \theta_{-k}\left|K^r_{2,i}\right|^2 \sigma^2_{x_{-k,i}}\right) \left(\left|K^r_{1,i}\right|^2 \sigma^2_{w_{k,i}} + \left|K^r_{2,i}\right|^2 \sigma^2_{w_{-k,i}}\right) \\ & + 2a_i^2 \left(\tilde{\theta}_k |\xi_{1,i}|^2 \sigma^2_{s_{k,i}} + \tilde{\theta}_{-k} |\xi_{2,i}|^2 \sigma^2_{s_{-k,i}}\right) \left(\left|K^r_{1,i}\right|^2 \sigma^2_{w_{k,i}} + \left|K^r_{2,i}\right|^2 \sigma^2_{w_{-k,i}}\right) - \mu^2_\Theta \Big) \end{aligned} \quad (35)$$

where $P_{\mathrm{fa},i}$ and $P_{d,i}$ $(i \in \{1,\ldots,N_{\mathrm{su}}\})$ stand for the false alarm and detection probabilities of the ith SU, respectively.

Proof: See Appendix D. ■

Proposition 5: If the AND rule is employed, then the false alarm and detection probabilities can be expressed as

$$P_{C,\mathrm{fa}} = \prod_{i=1}^{N_{\mathrm{su}}} P_{\mathrm{fa},i} \tag{46}$$

$$P_{C,d} = \prod_{i=1}^{N_{\mathrm{su}}} P_{d,i} \tag{47}$$

where $P_{\mathrm{fa},i}$ and $P_{d,i}$ $(i \in \{1,2\})$ stand for the false alarm and detection probabilities of the ith SU, respectively.

Proof: See Appendix E. ■

Proposition 6: If the MAJORITY rule is employed, then the false alarm and detection probabilities can be expressed as

$$P_{C,\mathrm{fa}} = \sum_{i=1}^{\mathrm{card}(\mathcal{D})} U\left(\sum_{l=1}^{N_{\mathrm{su}}} d_{l,k} - \left\lceil \frac{N_{\mathrm{su}}}{2} \right\rceil\right) \times \prod_{j=1}^{N_{\mathrm{su}}} \left(U(-d_{j,k})(1-P_{\mathrm{fa},j}) + U(d_{j,k}-1)P_{\mathrm{fa},j}\right) \tag{48}$$

$$P_{C,d} = \sum_{i=1}^{\mathrm{card}(\mathcal{D})} U\left(\sum_{l=1}^{N_{\mathrm{su}}} d_{l,k} - \left\lceil \frac{N_{\mathrm{su}}}{2} \right\rceil\right) \times \prod_{j=1}^{N_{\mathrm{su}}} \left(U(-d_{j,k})(1-P_{d,j}) + U(d_{j,k}-1)P_{d,j}\right) \tag{49}$$

where $P_{\mathrm{fa},i}$ and $P_{d,i}$ represent the false alarm and detection probabilities of the ith SU, respectively. Moreover, $\mathcal{D} = [d_1, d_2, \ldots, d_{N_{\mathrm{su}}}]$ denotes the SUs' decision set, where $d_i = 0$ and $d_i = 1$, $i = 1,\ldots,N_{\mathrm{su}}$, stand for the absence and the presence of PU activity at the sensing channel, respectively.

Proof: See Appendix F. ■

V. Numerical and Simulation Results

Here, we demonstrate the effects of IQI on the spectrum sensing performance of the EDs by illustrating numerical and simulation results for different IQI and SIS levels. Each of the reported figures contains both analytical and simulation results, which are represented by lines and discrete marks, respectively.

A. Single-Channel Energy Detector

In the case of the single-channel ED, we consider the following insightful scenario. The SNR of the received ideal signal at the SU i, $i \in \{1,2\}$, due to the PU activity is -15 dB, whereas before applying an SIS technique, the self-interference-to-noise ratio (INR) due to the transmission of the SU i is set to 20 dB. We assume that both TX and RX suffer from the same level of IQI and the degree of SIS is set to 0.01 (i.e., 40 dB). Furthermore, the ED is assumed to use $N_s = 8 \times 10^3$ samples.

In Fig. 2, the false alarm probability is plotted against the energy detection threshold, for different values of IRR. It

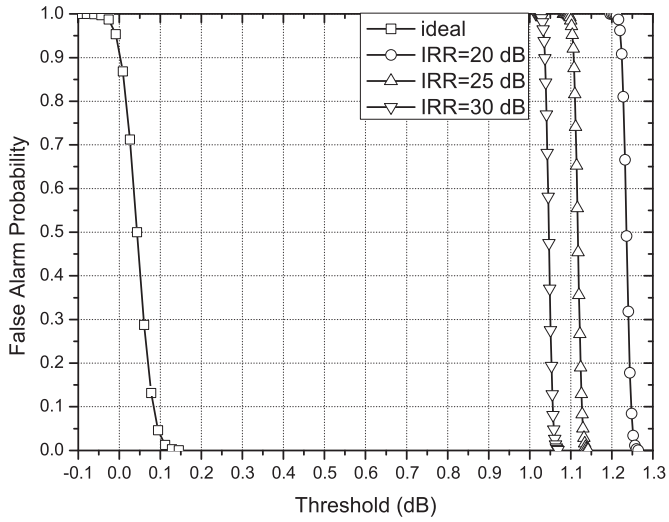

Fig. 2. False alarm probability as a function of the energy threshold for different values of IRR and $a_1 = a_2 = 0.01$.

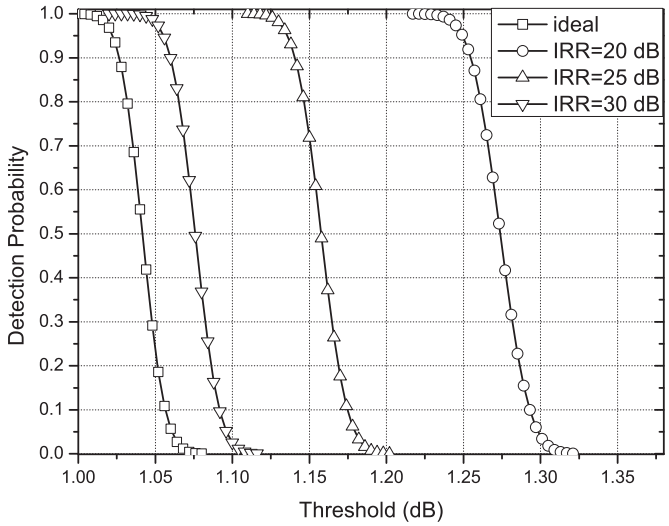

Fig. 3. Detection probability as a function of the energy threshold for different values of IRR and $a_1 = a_2 = 0.01$.

becomes evident from the figure that the analytical results are identical with the simulation results, thus verifying the presented analytical framework. Moreover, it is observed that, as IRR decreases, the self-interference due to IQI increases; consequently, to achieve a target false alarm probability, the energy threshold should be increased. For instance, if the target false alarm probability threshold is equal to 0.1, then in the case of ideal RF front end, the energy threshold should be set to 0.85 dB. When a nonideal CR device with IRR = 25 dB is considered, it should be shifted by about 0.2 dB and be set to 1.05 dB. This may not seem to be a significant shift; however, if the effects of IQI are not taken into consideration, the false alarm probability of the system will be equal to 1. This observation indicates the importance of the derived expressions.

Fig. 3 illustrates the impact of IQI in the detection performance of the FD CR devices. Specifically, the detection probability is plotted against the energy threshold for different levels of IQI. We observe that, as IRR decreases, the interference, due

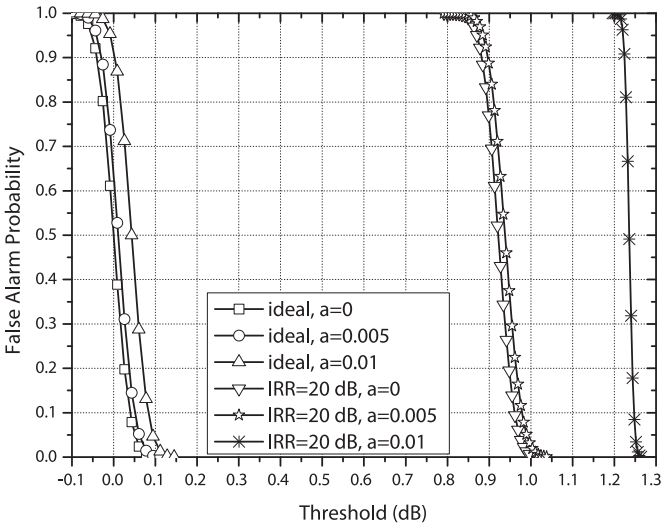

Fig. 4. False alarm probability as a function of the energy threshold for different values of IRR and a.

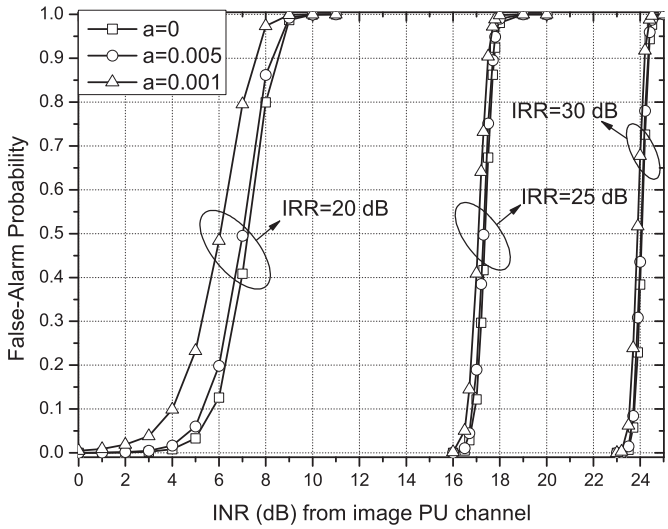

Fig. 5. False alarm probability as a function of the INR caused by the activity at the image PU channel for different values of IRR and levels of SIS when $\theta_{-k} = \tilde{\theta}_{-k} = \tilde{\theta}_k = 1$.

to IQI and partial SIS, increases, and, consequently, for a given energy threshold, the detection probability increases. For example, for $\gamma = 1.05$ dB and considering ideal RF front end, the detection probability is about 0.2. On the other hand, in the case of I/Q imbalanced RF front end with IRR $= 25$ dB and for the same energy threshold, the detection probability is equal to 1. Additionally, if the target false alarm probability is set to 0.1, then in the case of ideal RF front end, the corresponding detection probability is equal to 1, whereas in the case of nonideal RF front end with IRR $= 20$ dB, the energy threshold should be set to 1.257 dB, and the corresponding detection probability is 0.87. This example indicates that the spectrum sensing capabilities of the FD CR ED are constrained due to IQI.

In Fig. 4, the false alarm probability is illustrated as a function of the energy detection threshold for different IRR and a values. Note that the curve denoted by "ideal, $a = 0$" corresponds to special case 2, whereas the curves denoted by "ideal, $a = 0.005$" and "ideal, $a = 0.01$" correspond to special case 1. Moreover, the curves denoted by "IRR $= 20$ dB, $a = 0$" correspond to special case 3. It becomes evident from this figure that the analytical results presented in the special cases in Section III are identical with the simulation results, thus verifying the presented analytical framework. Additionally, we observe that, for a given IRR, as a increases, the false alarm probability increases. For example, for an energy threshold equal to 0.99 dB, IRR $= 20$ dB, and $a = 0$, the false alarm probability is about 0.1. However, if a increases to 0.01, the false alarm probability becomes 1. This indicates the importance of taking into consideration the impact of partial SIS when selecting the energy threshold. Finally, by comparing the spectrum sensing performance affected by IQI and partial SIS, it becomes apparent that the impact of IQI to the spectrum sensing performance is more detrimental than the impact of partial SIS.

B. Multichannel Energy Detector

In the case of the multichannel ED, it is assumed that there are eight channels and that the second channel is sensed $(k=2)$. The signal and total guard band bandwidths are assumed to be 9 MHz and 125 kHz, respectively. The noise variance for all channels is assumed to be equal to 1. Unless otherwise stated, the SNR of the received ideal signal at the SU i, $i \in \{1, 2\}$ at $k = 2$, due to the PU activity is -15 dB, whereas the INR of the PU mirror channel $(k = -2)$ is 15 dB. We also consider that, before applying any SIS technique, the INR due to the transmission of the SU i is set to 20 dB for both $k = 2$ and $k = -2$ channels. To determine the PU channel status, the ED is assumed to use $N_s = 8 \times 10^3$ samples.

In Fig. 5, the joint impact of IQI and partial SIS in the false alarm probability is demonstrated. Specifically, the false alarm probability against the INR caused by the activity at the image PU channel for different values of IRR and levels of SIS is presented in this figure for the worst-case scenario in which $\theta_{-k} = \tilde{\theta}_{-k} = \tilde{\theta}_k = 1$. Note that the energy detection threshold is set to 1.14 dB, i.e., $\gamma \approx 1.14$ dB. Furthermore, as a benchmark, we consider the ideal RF front end case with perfect SIS and $\gamma \approx 1.14$ dB, where the false alarm probability is practically set to zero. As expected, for fixed IRR and a, as the INR from the image PU signal increases, the interference from the mirror channels increases, which, consequently, increases the false alarm probability. Moreover, for given a and INR from the image PU signal value, as IRR increases, the leakage from the image PU channel decreases, resulting in the decrease of the false alarm probability. For given IRR and INR from the image PU signal values, as a increases, the leakage from the transmitted channels k and $-k$ increases, which increases the false alarm probability. For example, for INR $= 6$ dB and IRR $= 20$ dB, the increase of a from 0.005 to 0.01 leads to about 145% increase of the false alarm probability.

In Figs. 6 and 7, the joint impact of IQI and partial SIS in the detection probability is demonstrated. Specifically, in Fig. 6, the detection probability is plotted against the SNR for different interference channel occupancy sets, i.e., $\Theta_I = [\theta_{-k}, \tilde{\theta}_k, \tilde{\theta}_{-k}]$, when the energy detection threshold is $\gamma \approx 1.14$ dB, the level of SIS is set to -40 dB, IRR $= 20$ dB, $\phi = 3^\circ$, and the INR caused

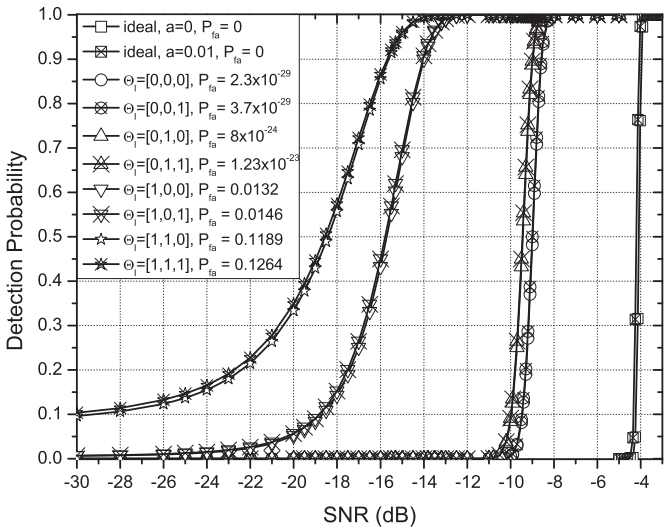

Fig. 6. Detection probability as a function of the SNR for different $\Theta_I = [\theta_{-k}, \tilde{\theta}_k, \tilde{\theta}_{-k}]$ when IRR $= 20$ dB and $a = 0.001$.

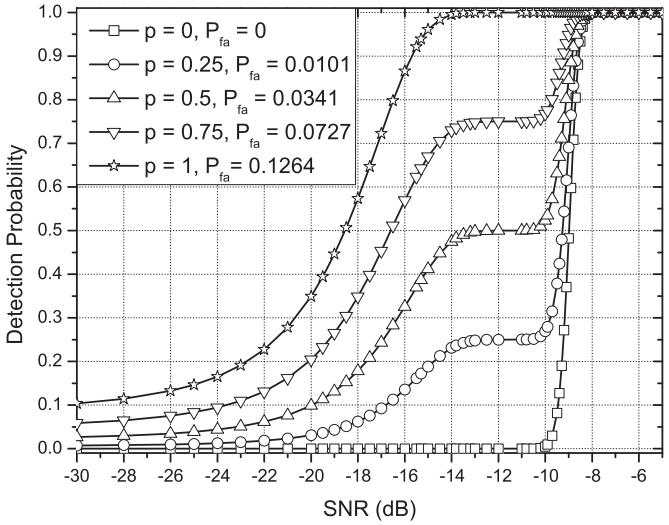

Fig. 7. Detection probability as a function of the SNR for different values of $p = p_{-k} = \tilde{p}_{-k} = \tilde{p}_k$ when IRR $= 20$ dB and $a = 0.001$.

by the activity at the image PU channel is 10 dB. For each interference channel occupancy set, the corresponding false alarm probabilities are reported in the legend. As a benchmark, the detection probability of an ideal RF front-end transceiver with $a = 0$ and $a = 0.01$ is also illustrated. As expected, for a given Θ_I, as SNR increases, the detection probability increases. Furthermore, it is observed that, for a given SNR, the detection probability increases as the interference increases. However, this comes with an inevitable price of increased false alarm probability and hence a dramatic decrease in the ability to identify vacant spectrum. For example, for SNR $= -20$ dB and $\Theta_I = [1, 0, 1]$, the detection and false alarm probabilities are 0.5638 and 0.0146, respectively, whereas for the same SNR and $\Theta_I = [1, 1, 1]$, the detection and false alarm probabilities are 0.34902 and 0.1264, respectively. In addition, since the leakage to the sensed channel k from the transmitted signal at the channel $-k$ is about -20 dB due to IQI and -40 dB due

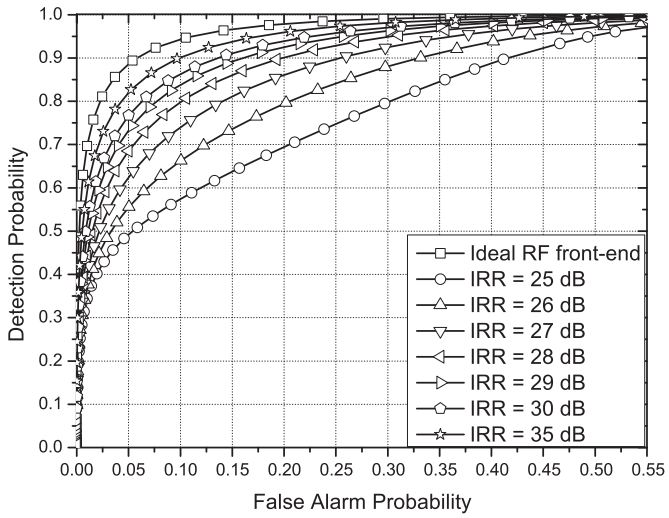

Fig. 8. ROCs for different values of IRR, when $p_{-k} = \tilde{p}_{-k} = \tilde{p}_k = 0.5$, $a = 0.01$, SNR $= -15$ dB, and the INR caused by the activity at the image PU channel is equal to 10 dB.

to the employed SIS technique, the signal leakage to channel k from the signal transmitted at channel k due to the joint effect of IQI and SIS is about -60 dB. Consequently, the leakage from the signal transmitted at channel $-k$ does not significantly affect the spectrum sensing capabilities of the multichannel ED.

Fig. 7 presents the detection probability as a function of SNR for different values of $p = p_{-k} = \tilde{p}_{-k} = \tilde{p}_k$ when the energy detection threshold is $\gamma \approx 1.14$ dB, the level of SIS is set to -40 dB, IRR $= 20$ dB, $\phi = 3^\circ$, and the INR caused by the activity at the image PU channel is set to 10 dB, whereas the INR due to the transmission of the SU at both channels k and $-k$ is set to 20 dB. For each interference channel occupancy set, the corresponding false alarm probabilities are reported in the legend. It is observed that, as p increases, the probability of channel leakage from the received signal at channel k and the transmitted signals at channels k and $-k$ increases, and therefore, the detection probability also increases. However, this comes at the expense of increasing the false alarm probability. Furthermore, for SNR values in the range of $[-14, -10$ dB$]$ and a given p, the detection probability remains constant. This can be explained using Fig. 6, where the contributions of the channel occupancy sets $\Theta_I = [0, 1, 0]$ and $\Theta_I = [0, 1, 1]$ are observed after -10 dB, whereas the contributions of the remaining channel occupancy sets are observed after -14 dB. Therefore, for SNR values in the range of $[-14, -10$ dB$]$ and a given p, the detection probability remains constant.

In Fig. 8, ROCs are presented for different values of IRR, when $p_{-k} = \tilde{p}_{-k} = \tilde{p}_k = 0.5$, $a = 0.001$, the SNR is set to -15 dB, and the INR caused by the activity at the image PU channel is set to 10 dB, whereas the INR due to the transmission of the SU at both channels k and $-k$ is set to 20 dB. Again, the detrimental effects of IQI and partial SIS on the CR ED's spectrum sensing capabilities are observed. For example, for $P_{\rm fa} = 0.1$ and IRR $= 25$ dB, the detection probability cannot exceed 0.6. However, in the case of ideal RF front end and perfect SIS, for the same $P_{\rm fa}$, the detection probability is about 0.9. In other words, the joint effects of IQI and imperfect SIS result

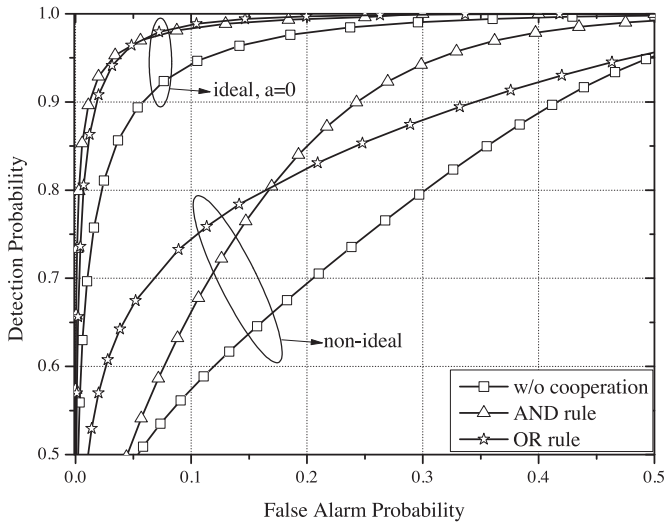

Fig. 9. ROCs for different decision rules when $p = p_{-k} = \tilde{p}_{-k} = \tilde{p}_k = 0.5$, IRR $= 25$ dB, and $a = 0.01$.

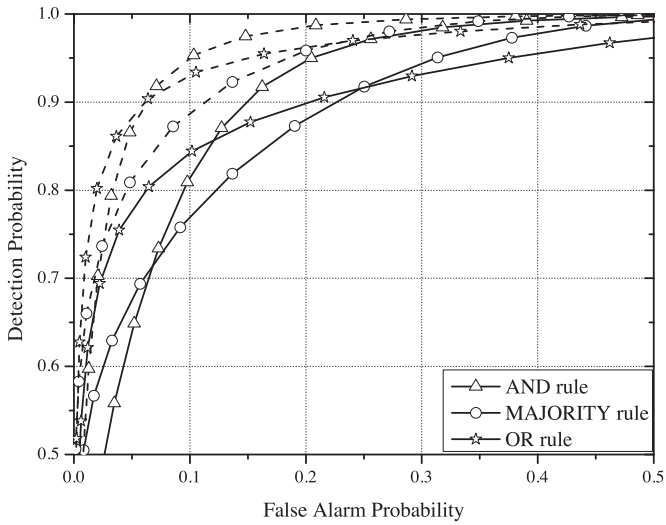

Fig. 10. ROCs for different decision rules when $p = p_{-k} = \tilde{p}_{-k} = \tilde{p}_k = 0.5$, IRR $= 30$ dB, $a = 0.01$, and (continuous lines) $N_{\rm su} = 3$ or (dashed lines) $N_{\rm su} = 5$.

in a degradation on the order of 50%. Furthermore, it is evident that, as IRR increases, the leakage from the image channels is constrained, and hence, the spectrum sensing capability of the EDs is improved.

C. Cooperative Sensing

In the case of cooperative sensing, we consider that each one of the two SUs employs a multichannel ED that downconverts eight channels ($K = 8$) and senses the second one ($k = 2$). Note that, in the case where only two SUs are involved, the MAJORITY rule coincides with the AND rule. The SNR of the received ideal signal at the SU i, $i \in \{1, 2\}$ at $k = 2$, due to the PU activity is -15 dB, whereas the INR of the PU mirror channel ($k = -2$) is 15 dB. We also consider that, before applying an SIS technique, the INR due to the transmission of the SU i is set to 20 dB in both $k = 2$ and $k = -2$ channels, $p_{-k} = \tilde{p}_{-k} = \tilde{p}_k = 0.5$, and $a = 0.001$. Again, the ED of each SU is assumed to use $N_s = 8 \times 10^3$ samples.

The ROCs corresponding to this scenario are plotted in Fig. 9, considering that the SUs employ the AND or the OR rule. As benchmarks, we also present the ideal case ROC, i.e., IRR $\to \infty$ and $a = 0$, and the ideal and nonideal ROCs, when the SUs do not use cooperative sensing. It is observed that the joint effects of IQI and partial SIS constrain the spectrum sensing capabilities for both cases of noncooperative and cooperative sensing. For instance, for $P_{\rm fa} = 0.1$, the detection probabilities in the case of ideal RF front end and perfect SIS in the case of individual sensing, cooperative sensing using AND rule, and cooperative sensing using OR rule are 0.94, 0.98, and 0.99, respectively. In the case of nonideal RF front end and partial SIS for $P_{\rm fa} = 0.1$, the corresponding probabilities are 0.58, 0.68, and 0.75. In other words, for $P_{\rm fa} = 0.1$, the spectrum sensing capability of the ED that uses the AND (OR) rule is reduced by 44.12% (32%), due to the effects of IQI and partial SIS. Furthermore, we observe that both the presented cooperative sensing schemes outperform the corresponding individual sensing scheme. However, the joint effects of IQI and partial SIS are so detrimental, even with the use of cooperative sensing; the performance of nonideal cooperative sensing is worse than that of the individual sensing CR system with ideal RF front end and perfect SIS. Moreover, in the case of ideal RF front end and perfect SIS, we observe that, in terms of spectrum sensing performance, systems that employ the OR rule outperform those that employ the AND rule, irrespective of the false alarm probability range. In the case of IRR $= 25$ dB and $a = 0.01$, the OR rule outperforms the AND rule for $P_{\rm fa} \in [0, 0.16941]$, whereas the AND rule outperforms the OR rule for $P_{\rm fa} \in (0.16941, 1]$.

In Fig. 10, ROCs are demonstrated for different values of $N_{\rm su}$, considering that the SUs employ the AND, the MAJORITY, or the OR rule and the SUs' RXs have the same IRR, which is equal to 30 dB. As expected, for a fixed decision rule, as $N_{\rm su}$ increases, the spectrum sensing capability of the EDs is improved. Moreover, it is observed that, for fixed $N_{\rm su}$, in the low-false-alarm regime, systems that employ the OR rule outperform those that employ the MAJORITY and AND rules. However, as the requirement for low false alarm probability is relaxed, the AND rule outperforms both the MAJORITY and OR rules. This indicates the importance of taking into consideration $N_{\rm su}$, the IQI levels, and the targeted false alarm probability, to select the decision rule that maximizes the spectrum sensing performance of the ED.

VI. Conclusion

This paper has investigated the spectrum sensing performance of opportunistic spectrum access FD CR system in both single- and multichannel EDs, when the SUs' devices employ SIS techniques and suffer from joint TX/RX IQI. We derived closed-form expressions for the false alarm and detection probabilities under realistic scenarios of nonperfect SIS and transceivers' RF front-end impairments, as well as for the theoretical scenarios of ideal RF front end and/or perfect SIS. Our results illustrated the degrading joint effects of IQI and partial SIS on the ED spectrum sensing performance, which result in

significant losses in spectrum utilization. Specifically, in the case of single-channel EDs, we observed that the negligence of IQI and partial SIS can lead to a wrong choice of the energy threshold, which may result in a dramatic increase of the false alarm probability, while, at the same time, the detection probability might significantly decrease. Moreover, in the case of multichannel EDs, partial SIS and IQI cause self-interference and mirror interference that appreciably restrict the ED's capabilities. Hence, when designing FD CR devices, whether a single- or a multichannel ED is employed, IQI and partial SIS should be carefully taken into consideration. Finally, we extended the analysis in case of cooperative sensing to observe that, even with the use of cooperative schemes, it is impossible to fully compensate for the joint effects of IQI and partial SIS.

APPENDIX A
PROOF OF PROPOSITION 1

Since N_s is sufficiently large, the central limit theorem [41] can be applied. In this case, the test statistics follows a Gaussian distribution with mean and variance that are, respectively, given by

$$\mu_\theta = E[T_i|\theta] = \frac{1}{N_s} E\left[\sum_{n=0}^{N_s-1} |y_i(n)|^2\right] = E\left[|y_i(n)|^2\right] \quad (50)$$

$$\sigma_\theta^2 = \mathrm{Var}[T_i|\theta] = \frac{1}{N_s}\left(E\left[|y_i|^4\right] - \mu_\theta^2\right). \quad (51)$$

Taking into consideration that x_i, s_i, and w_i are uncorrelated random variables, (50) can be rewritten as

$$\mu_\theta = \theta E\left[|x_i|^2\right] + a_i^2 E\left[|s_i|^2\right] + E\left[|w_i|^2\right]. \quad (52)$$

Moreover, since $x_{\mathrm{id},i}$, $s_{\mathrm{id},i}$, and $w_{\mathrm{id},i}$ are zero-mean CSCWG processes with uncorrelated real and imaginary parts with variances $\sigma^2_{x_{\mathrm{id},i}} = [|x_{\mathrm{id},i}|^2]$, $\sigma^2_{s_{\mathrm{id},i}} = E[|s_{\mathrm{id},i}|^2]$, and $\sigma^2_{w_{\mathrm{id},i}} = [|w_{\mathrm{id},i}|^2]$, respectively, the terms x_i, s_i, and w_i in (2)–(4) are random uncorrelated processes with variances that are given by

$$E\left[|x_i|^2\right] = \left(\left|K_{1,i}^r\right|^2 + \left|K_{2,i}^r\right|^2\right)\sigma^2_{x_{\mathrm{id},i}} \quad (53)$$

$$E\left[|s_i|^2\right] = \left(|\xi_{1,i}|^2 + |\xi_{2,i}|^2\right)\sigma^2_{s_{\mathrm{id},i}} \quad (54)$$

$$E\left[|w_i|^2\right] = \left(\left|K_{1,i}^r\right|^2 + \left|K_{2,i}^r\right|^2\right)\sigma^2_{w_{\mathrm{id},i}} \quad (55)$$

respectively. Substituting (53)–(55) into (52) and after some algebraic manipulations, we obtain (16).

Nevertheless, to derive the variance of the test statistics, we need to evaluate $E[|y_i|^4]$, which can be obtained using (1) as follows:

$$\begin{aligned} E\left[|y_i|^4\right] &= \theta E\left[|x_i|^4\right] + a_i^4 E\left[|s_i|^4\right] + E\left[|w_i|^4\right] \\ &\quad + 2a_i^2\theta E\left[|x_i|^2\right] E\left[|s_i|^2\right] + 2\theta E\left[|x_i|^2\right] E\left[|w_i|^2\right] \\ &\quad + 2a_i^2 E\left[|s_i|^2\right] E\left[|w_i|^2\right] \\ &\quad + 4E\left[\left(\Re\left\{\theta a_i x_i s_i^* + \theta x_i w_i^* + a_i s_i w_i^*\right\}\right)^2\right] \end{aligned} \quad (56)$$

where, according to (2)–(4), $E[|x_i|^4]$, $E[|s_i|^4]$, $E[|w_i|^4]$, and $E[(\Re\{\theta a_i x_i s_i^* + \theta x_i w_i^* + a_i s_i w_i^*\})^2]$ can be expressed as $E[|x_i|^4] = 2k_r\sigma^4_{x_{\mathrm{id},i}}$, $E[|s_i|^4] = 2k_{t,r}\sigma^4_{s_{\mathrm{id},i}}$, $E[|w_i|^4] = 2k_r\sigma^4_{w_{\mathrm{id},i}}$, and

$$\begin{aligned} &E\left[\left(\Re\left\{\theta a_i x_i s_i^* + \theta x_i w_i^* + a_i s_i w_i^*\right\}\right)^2\right] \\ &= \theta a_i^2 E\left[\Re\{x_i\}^2\right] E\left[\Re\{s_i\}^2\right] + a_i^2\theta E\left[\Im\{x_i\}^2\right] E\left[\Im\{s_i\}^2\right] \\ &\quad + \theta E\left[\Re\{x_i\}^2\right] E\left[\Re\{w_i\}^2\right] + \theta E\left[\Im\{x_i\}^2\right] E\left[\Im\{w_i\}^2\right] \\ &\quad + a_i^2 E\left[\Re\{s_i\}^2\right] E\left[\Re\{w_i\}^2\right] + a_i^2 E\left[\Im\{s_i\}^2\right] E\left[\Im\{w_i\}^2\right]. \end{aligned} \quad (57)$$

Next, we derive $E[\Re\{x_i\}^2]$, $E[\Re\{s_i\}^2]$, $E[\Re\{w_i\}^2]$, $E[\Im\{x_i\}^2]$, $E[\Im\{s_i\}^2]$, and $E[\Im\{w_i\}^2]$. By using (9), (11), and the fact that $E[\Re\{x_{\mathrm{id},i}\}^2] = E[\Im\{x_{\mathrm{id},i}\}^2] = \sigma^2_{x_{\mathrm{id}}}/2$, $E[\Re\{s_{\mathrm{id},i}\}^2] = E[\Im\{s_{\mathrm{id},i}\}^2] = \sigma^2_{s_{\mathrm{id}}}/2$, and $E[\Re\{w_{\mathrm{id},i}\}^2] = E[\Im\{w_{\mathrm{id},i}\}^2] = \sigma^2_{w_{\mathrm{id}}}/2$, we obtain

$$E\left[\Re\{x_i\}^2\right] = \frac{\sigma^2_{x_{\mathrm{id}}}}{2} \quad (58)$$

$$E\left[\Re\{s_i\}^2\right] = \frac{\sigma^2_{s_{\mathrm{id}}}}{2} \quad (59)$$

$$E\left[\Re\{w_i\}^2\right] = \frac{\sigma^2_{w_{\mathrm{id}}}}{2} \quad (60)$$

$$E\left[\Im\{x_i\}^2\right] = \left(\left(2\Re\left\{K_{1,i}^r\right\} - 1\right)^2 + 4\Im\left\{K_{1,i}^r\right\}^2\right)\frac{\sigma^2_{x_{\mathrm{id}}}}{2} \quad (61)$$

$$E\left[\Im\{s_i\}^2\right] = \left(\left(2\Re\left\{\xi_{1,i}\right\} - 1\right)^2 + 4\Im\{\xi_{1,i}\}^2\right)\frac{\sigma^2_{s_{\mathrm{id}}}}{2} \quad (62)$$

$$E\left[\Im\{w_i\}^2\right] = \left(\left(2\Re\left\{K_{1,i}^r\right\} - 1\right)^2 + 4\Im\left\{K_{1,i}^r\right\}^2\right)\frac{\sigma^2_{w_{\mathrm{id}}}}{2}. \quad (63)$$

Substituting (58)–(63) into (57) and then into (51) and (56), we obtain (17). This concludes the proof.

APPENDIX B
PROOF OF PROPOSITION 2

In the case of ideal RF front end, since $K_{1,i}^t = K_{1,i}^r = 1$ and $K_{2,i}^t = K_{2,i}^r = 0$, $y_{i|\theta} = \theta x_{\mathrm{id},i} + a s_{\mathrm{id},i} + w_{\mathrm{id},i}$. Furthermore, since $x_{\mathrm{id},i} \sim \mathcal{CN}(0, \sigma^2_{x_{\mathrm{id},i}})$, $s_{\mathrm{id},i} \sim \mathcal{CN}(0, \sigma^2_{s_{\mathrm{id},i}})$, and $w_{\mathrm{id},i} \sim \mathcal{CN}(0, \sigma^2_{w_{\mathrm{id},i}})$, $y_i(n)$ follows zero-mean complex Gaussian random distribution with a variance given by (31). Additionally, since T_i is the sum of zero-mean Gaussian processes, it follows chi-square distribution with $2N_s$ degrees of freedom and a cdf shown in (30). This concludes the proof.

APPENDIX C
PROOF OF PROPOSITION 3

Since N_s is sufficiently large, using the central limit theorem [41], the test statistics follow Gaussian distribution with the following mean and variance:

$$\mu_\Theta = E[T_i|\Theta] = \frac{1}{N_s} E\left[\sum_{n=0}^{N_s-1} |y_{i,k}(n)|^2\right] = E\left[|y_{i,k}(n)|^2\right] \quad (64)$$

$$\sigma_\theta^2 = \mathrm{Var}[T_i|\Theta] = \frac{1}{N_s}\left(E\left[|y_{i,k}|^4\right] - \mu_\Theta^2\right). \quad (65)$$

Taking into consideration that $x_{i,k}$, $x_{i,-k}$, $s_{i,k}$, $s_{i,-k}$, and $w_{i,k}$, $w_{i,-k}$ are uncorrelated random variable, (64) yields (34).

Moreover, based on (65), to evaluate the variance of the test statistics, we need to derive $E[|y_{i,k}|^4]$, which can be expressed as

$$\begin{aligned} E\left[|y_{i,k}|^4\right] &= E\left[\left(x_{\mathrm{IQI}} + a_i s_{\mathrm{IQI}} + w_{\mathrm{IQI}}\right)^4\right] \\ &= E\left[|x_{\mathrm{IQI}}|^4\right] + a_i^4 E\left[|s_{\mathrm{IQI}}|^4\right] + E\left[|w_{\mathrm{IQI}}|^4\right] \\ &\quad + 4E\left[\left(\Re\left\{a_i x_{\mathrm{IQI}} s_{\mathrm{IQI}}^* + x_{\mathrm{IQI}} w_{\mathrm{IQI}}^* + a_i s_{\mathrm{IQI}} w_{\mathrm{IQI}}^*\right\}\right)^2\right] \end{aligned} \tag{66}$$

where $x_{\mathrm{IQI}} = \theta_k K_{1,i}^r x_{i,k}(n) + \theta_{-k} K_{2,i}^r x_{i,-k}^*(n)$, $s_{\mathrm{IQI}} = \tilde{\theta}_k a_i \xi_{1,i} s_{i,k}(n) + \tilde{\theta}_{-k} a_i \xi_{2,i} s_{i,-k}^*(n)$, and $w_{\mathrm{IQI}} = K_{1,i}^r w_{i,k}(n) + K_{2,i}^r w_{i,-k}^*(n)$. Therefore

$$\begin{aligned} E\left[|x_{\mathrm{IQI}}|^4\right] &= 2\theta_k \left|K_{1,i}^r\right|^4 \sigma_{x_{i,k}}^4 + 2\theta_{-k} \left|K_{2,i}^r\right|^4 \sigma_{x_{i,-k}}^4 \\ &\quad + 2\theta_k \theta_{-k} \left(\left|K_{1,i}^r\right|^2 \left|K_{2,i}^r\right|^2 + \alpha^2 + \beta^2\right) \sigma_{x_{i,k}}^2 \sigma_{x_{i,-k}}^2 \end{aligned} \tag{67}$$

$$\begin{aligned} E\left[|s_{\mathrm{IQI}}|^4\right] &= 2\tilde{\theta}_k |x i_{1,i}|^4 \sigma_{s_{i,k}}^4 + 2\tilde{\theta}_{-k} |\xi_{2,i}|^4 \sigma_{s_{i,-k}}^4 \\ &\quad + 2\tilde{\theta}_k \tilde{\theta}_{-k} \left(|\xi_{1,i}|^2 |\xi_{2,i}|^2 + \delta^2 + \zeta^2\right) \sigma_{s_{i,k}}^2 \sigma_{s_{i,-k}}^2 \end{aligned} \tag{68}$$

$$\begin{aligned} E\left[|w_{\mathrm{IQI}}|^4\right] &= 2\left|K_{1,i}^r\right|^4 \sigma_{w_{i,k}}^4 + 2\left|K_{2,i}^r\right|^4 \sigma_{w_{i,-k}}^4 \\ &\quad + 2\left(\left|K_{1,i}^r\right|^2 \left|K_{2,i}^r\right|^2 + \alpha^2 + \beta^2\right) \sigma_{w_{i,k}}^2 \sigma_{w_{i,-k}}^2. \end{aligned} \tag{69}$$

Furthermore, we can easily prove that x_{IQI}, s_{IQI}, and w_{IQI} are zero-mean uncorrelated random processes. Consequently, $E[(\Re\{a_i x_{\mathrm{IQI}} s_{\mathrm{IQI}}^* + x_{\mathrm{IQI}} w_{\mathrm{IQI}}^* + a_i s_{\mathrm{IQI}} w_{\mathrm{IQI}}^*\})^2]$ can be expressed as

$$\begin{aligned} &E\left[\left(\Re\left\{a_i x_{\mathrm{IQI}} s_{\mathrm{IQI}}^* + x_{\mathrm{IQI}} w_{\mathrm{IQI}}^* + a_i s_{\mathrm{IQI}} w_{\mathrm{IQI}}^*\right\}\right)^2\right] \\ &\quad = a_i^2 E\left[\left(\Re\{x_{\mathrm{IQI}}\}\right)^2\right] E\left[\left(\Re\{s_{\mathrm{IQI}}\}\right)^2\right] \\ &\qquad + a_i^2 E\left[\left(\Im\{x_{\mathrm{IQI}}\}\right)^2\right] E\left[\left(\Im\{s_{\mathrm{IQI}}\}\right)^2\right] \\ &\qquad + E\left[\left(\Re\{x_{\mathrm{IQI}}\}\right)^2\right] E\left[\left(\Re\{w_{\mathrm{IQI}}\}\right)^2\right] \\ &\qquad + E\left[\left(\Im\{x_{\mathrm{IQI}}\}\right)^2\right] E\left[\left(\Im\{w_{\mathrm{IQI}}\}\right)^2\right] \\ &\qquad + a_i^2 E\left[\left(\Re\{s_{\mathrm{IQI}}\}\right)^2\right] E\left[\left(\Re\{w_{\mathrm{IQI}}\}\right)^2\right] \\ &\qquad + a_i^2 E\left[\left(\Im\{s_{\mathrm{IQI}}\}\right)^2\right] E\left[\left(\Im\{w_{\mathrm{IQI}}\}\right)^2\right]. \end{aligned} \tag{70}$$

Additionally, since $\Re\{x_{i,k}\}$, $\Im\{x_{i,k}\}$, $\Re\{x_{i,-k}\}$, $\Im\{x_{i,-k}\}$, $\Re\{s_{i,k}\}$, $\Im\{s_{i,k}\}$, $\Re\{s_{i,-k}\}$, $\Im\{s_{i,-k}\}$, $\Re\{w_{i,k}\}$, $\Im\{w_{i,k}\}$, $\Re\{w_{i,-k}\}$, and $\Im\{w_{i,-k}\}$ are uncorrelated random processes, we show that

$$\begin{aligned} E\left[\left(\Re\{x_{\mathrm{IQI}}\}\right)^2\right] &= E\left[\left(\Im\{x_{\mathrm{IQI}}\}\right)^2\right] \\ &= \theta_k \left|K_{1,i}^r\right|^2 \frac{\sigma_{x_{k,i}}}{2} + \theta_{-k} \left|K_{2,i}^r\right|^2 \frac{\sigma_{x_{-k,i}}}{2} \end{aligned} \tag{71}$$

$$\begin{aligned} E\left[\left(\Re\{s_{\mathrm{IQI}}\}\right)^2\right] &= E\left[\left(\Im\{s_{\mathrm{IQI}}\}\right)^2\right] \\ &= \tilde{\theta}_k |\xi_{1,i}|^2 \frac{\sigma_{s_{k,i}}}{2} + \tilde{\theta}_{-k} |\xi_{2,i}|^2 \frac{\sigma_{s_{-k,i}}}{2} \end{aligned} \tag{72}$$

$$\begin{aligned} E\left[\left(\Re\{w_{\mathrm{IQI}}\}\right)^2\right] &= E\left[\left(\Im\{w_{\mathrm{IQI}}\}\right)^2\right] \\ &= \left|K_{1,i}^r\right|^2 \frac{\sigma_{w_{k,i}}}{2} + \left|K_{2,i}^r\right|^2 \frac{\sigma_{w_{-k,i}}}{2}. \end{aligned} \tag{73}$$

By substituting (71)–(73) into (70) and then by substituting this result and (67)–(69) into (65), we obtain (35). This concludes the proof.

Appendix D
Proof of Proposition 4

When the OR rule is employed, the false alarm probability can be expressed as

$$\begin{aligned} P_{C,\mathrm{fa}} = P_r\left(\{T_1 > \gamma_1\} \cup \{T_2 > \gamma_2\}\right. \\ \left. \cup \cdots \cup \{T_{N_{\mathrm{su}}} > \gamma_{N_{\mathrm{su}}}\} | \theta = 0\right) \end{aligned} \tag{74}$$

or, equivalently, as

$$\begin{aligned} P_{C,\mathrm{fa}} = 1 - P_r\left(\{T_1 < \gamma_1\} \cup \{T_2 < \gamma_2\}\right. \\ \left. \cup \cdots \cup \{T_{N_{\mathrm{su}}} < \gamma_{N_{\mathrm{su}}}\} | \theta = 0\right). \end{aligned} \tag{75}$$

In (75), T_i and $\gamma_i (i \in \{1, 2, \ldots, N_{\mathrm{su}}\})$ stand for the energy statistics and the energy threshold of the ith SU. Since the N_{su} SUs decide independently whether the sensing channel is occupied, (75) yields (44). Similarly, we can prove (45). This concludes the proof.

Appendix E
Proof of Proposition 5

When the AND rule is employed, the false alarm probability can be obtained as

$$\begin{aligned} P_{C,\mathrm{fa}} = P_r\left(\{T_1 > \gamma_1\} \cap \{T_2 > \gamma_2\right. \\ \left. \cap \cdots \cap \{T_{N_{\mathrm{su}}} > \gamma_{N_{\mathrm{su}}}\} | \theta = 0\right). \end{aligned} \tag{76}$$

In (76), T_i and $\gamma_i (i \in \{1, \ldots, N_{\mathrm{su}}\})$ stand for the energy statistics and the energy threshold of the ith SU. Since the SUs independently decide whether the sensing channel is occupied, (76) can be rewritten as (46). Similarly, we can prove that the detection probability is given by (47). This concludes the proof.

Appendix F
Proof of Proposition 6

If the sensing channel is idle ($\theta = 0$), then the probability that the SU j reports that the channel is busy ($d_j = 1$) can be expressed as $P_{\mathrm{fa},j}$, whereas the probability that the SU j reports that the channel is idle ($d_j = 0$) is given by $(1 - P_{\mathrm{fa},j})$. Therefore, since each SU decides individually whether there is PU activity in the sensing channel, the probability that $\lceil N_{\mathrm{su}}/2 \rceil$

SUs report a fixed decision set $\mathcal{D} = [d_1, d_2, \ldots, d_{N_{\rm su}}]$, if $\theta_k = 0$, can be obtained as

$$P_{\rm fa}(\mathcal{D}) = \prod_{j=1}^{N_{\rm su}} \left(U(-d_j)(1 - P_{{\rm fa},j}) + U(d_j - 1)P_{{\rm fa},j}\right). \quad (77)$$

Furthermore, based on the MAJORITY rule, the sensing channel is considered busy if at least $\lceil N_{\rm su}/2 \rceil$ SUs reports "1." Consequently, for a given decision set $\mathcal{D}$, the false alarm probability can be evaluated by

$$P_{C,{\rm FA}|\mathcal{D}} = U\left(\sum_{l=1}^{N_{\rm su}} d_l - k_{\rm su}\right) \times \prod_{j=1}^{n_{\rm su}} \left(U(-d_j)(1 - P_{{\rm fa},j}) + U(d_j - 1)P_{{\rm fa},j}\right). \quad (78)$$

Hence, for any possible $\mathcal{D}$, the false alarm probability, using the MAJORITY rule, can be obtained by (48). Similarly, we can prove that the detection probability is given by (49). This concludes the proof.

REFERENCES

[1] "Spectrum policy task force report," Fed. Commun. Comm. (FCC), Washington, DC, USA, Nov. 2002.

[2] J. Xiao, R. Hu, Y. Qian, L. Gong, and B. Wang, "Expanding LTE network spectrum with cognitive radios: From concept to implementation," *IEEE Wireless Commun. Mag.*, vol. 20, no. 2, pp. 12–19, Apr. 2013.

[3] M. Sherman, A. Mody, R. Martinez, C. Rodriguez, and R. Reddy, "IEEE standards supporting cognitive radio and networks, dynamic spectrum access, and coexistence," *IEEE Commun. Mag.*, vol. 46, no. 7, pp. 72–79, Jul. 2008.

[4] W. Afifi and M. Krunz, "Incorporating self-interference suppression for full-duplex operation in opportunistic spectrum access systems," *IEEE Trans. Wireless Commun.*, vol. 14, no. 4, pp. 2180–2191, Apr. 2015.

[5] T. Yucek and H. Arslan, "A survey of spectrum sensing algorithms for cognitive radio applications," *IEEE Commun. Surveys Tut.*, vol. 11, no. 1, pp. 116–130, Jan. 2009.

[6] O. Altrad, S. Muhaidat, A. Al-Dweik, A. Shami, and P. Yoo, "Opportunistic spectrum access in cognitive radio networks under imperfect spectrum sensing," *IEEE Trans. Veh. Technol.*, vol. 63, no. 2, pp. 920–925, Feb. 2014.

[7] L. Fan, X. Lei, T. Duong, R. Hu, and M. Elkashlan, "Multiuser cognitive relay networks: Joint impact of direct and relay communications," *IEEE Trans. Wireless Commun.*, vol. 13, no. 9, pp. 5043–5055, Sep. 2014.

[8] S. Huang, X. Liu, and Z. Ding, "Optimal sensing-transmission structure for dynamic spectrum access," in *Proc. IEEE INFOCOM*, Apr. 2009, pp. 2295–2303.

[9] A.-A. A. Boulogeorgos, N. D. Chatzidiamantis, and G. K. Karagiannidis, "Spectrum sensing with multiple primary users over fading channels," *IEEE Commun. Lett.*, vol. 20, no. 7, pp. 1457–1460, Jul. 2016.

[10] B. Razavi, "Cognitive radio design challenges and techniques," *IEEE J. Solid-State Circuits*, vol. 45, no. 8, pp. 1542–1553, Aug. 2010.

[11] V. Syrjala, M. Valkama, L. Anttila, T. Riihonen, and D. Korpi, "Analysis of oscillator phase-noise effects on self-interference cancellation in full-duplex OFDM radio transceivers," *IEEE Trans. Wireless Commun.*, vol. 13, no. 6, pp. 2977–2990, Jun. 2014.

[12] J. Li, M. Matthaiou, and T. Svensson, "I/Q imbalance in AF dual-hop relaying: Performance analysis in Nakagami-m fading," *IEEE Trans. Commun.*, vol. 62, no. 3, pp. 839–847, Mar. 2014.

[13] J. Li, M. Matthaiou, and T. Svensson, "I/Q imbalance in two-way AF relaying," *IEEE Trans. Commun.*, vol. 62, no. 7, pp. 2271–2285, Jul. 2014.

[14] M. Valkama, M. Renfors, and V. Koivunen, "Advanced methods for I/Q imbalance compensation in communication receivers," *IEEE Trans. Signal Process.*, vol. 49, no. 10, pp. 2335–2344, Oct. 2001.

[15] L. Anttila, M. Valkama, and M. Renfors, "Circularity-based I/Q imbalance compensation in wideband direct-conversion receivers," *IEEE Trans. Veh. Commun.*, vol. 57, no. 4, pp. 2099–2113, Jul. 2008.

[16] A. Gokceoglu, S. Dikmese, M. Valkama, and M. Renfors, "Energy detection under IQ imbalance with single- and multi-channel direct-conversion receiver: Analysis and mitigation," *IEEE J. Sel. Areas Commun.*, vol. 32, no. 3, pp. 411–424, Mar. 2014.

[17] A. Gokceoglu, Y. Zou, M. Valkama, and P. Sofotasios, "Multi-channel energy detection under phase noise: Analysis and mitigation," *Mobile Netw. Appl.*, vol. 19, no. 4, pp. 473–486, Aug. 2014.

[18] J. Verlant-Chenet, J. Renard, J.-M. Dricot, P. De Doncker, and F. Horlin, "Sensitivity of spectrum sensing techniques to RF impairments," in *Proc. IEEE 71st VTC—Spring*, May 2010, pp. 1–5.

[19] A. Zahedi-Ghasabeh, A. Tarighat, and B. Daneshrad, "Cyclo-stationary sensing of OFDM waveforms in the presence of receiver RF impairments," in *Proc. IEEE WCNC*, Apr. 2010, pp. 1–6.

[20] A. ElSamadouny, A. Gomaa, and N. Al-Dhahir, "Likelihood-based spectrum sensing of OFDM signals in the presence of Tx/Rx I/Q imbalance," in *Proc. IEEE GLOBECOM*, Dec. 2012, pp. 3616–3621.

[21] O. Semiari, B. Maham, and C. Yuen, "Effect of I/Q imbalance on blind spectrum sensing for OFDMA overlay cognitive radio," in *Proc. 1st IEEE ICCC*, Aug. 2012, pp. 433–437.

[22] A.-A. A. Boulogeorgos, N. Chatzidiamantis, G. K. Karagiannidis, and L. Georgiadis, "Energy detection under RF impairments for cognitive radio," in *Proc. IEEE CoCoNet ICC Workshops 16*, London, U.K., Jun. 2015, pp. 955–960.

[23] A.-A. A. Boulogeorgos, N. D. Chatzidiamantis, and G. K. Karagiannidis, "Energy detection spectrum sensing under RF imperfections," *IEEE Trans. Commun.*, vol. 64, no. 7, pp. 2754–2766, Jul. 2016.

[24] G. Zheng, I. Krikidis, and B. Ottersten, "Full-duplex cooperative cognitive radio with transmit imperfections," *IEEE Trans. Wireless Commun.*, vol. 12, no. 5, pp. 2498–2511, May 2013.

[25] I. S. Gradshteyn and I. M. Ryzhik, *Table of Integrals, Series, and Products*, 7th ed. New York, NY, USA: Academic, 2007.

[26] Y. Yuan, P. Bahl, R. Chandra, T. Moscibroda, and Y. Wu, "Allocating dynamic time-spectrum blocks in cognitive radio networks," in *Proc. 8th ACM Int. Symp. MobiHoc*, New York, NY, USA, Sep. 2007, pp. 130–139. [Online]. Available: http://doi.acm.org/10.1145/1288107.1288125

[27] H. Bany Salameh and M. Krunz, "Channel access protocols for multihop opportunistic networks: Challenges and recent developments," *IEEE Netw.*, vol. 23, no. 4, pp. 14–19, Jul. 2009.

[28] T. Schenk, *RF Imperfections in High-Rate Wireless Systems*. Eindhoven, The Netherlands: Springer-Verlag, 2008.

[29] S. Chatterjee, S. Maity, and T. Acharya, "Energy efficient cognitive radio system for joint spectrum sensing and data transmission," *IEEE J. Emerging Sel. Topics Circuits Syst.*, vol. 4, no. 3, pp. 292–300, Sep. 2014.

[30] B. Razavi, *RF Microelectronics*. Englewood Cliffs, NJ, USA: Prentice-Hall, 1998, vol. 1.

[31] S. Mirabbasi and K. Martin, "Classical and modern receiver architectures," *IEEE Commun. Mag.*, vol. 38, no. 11, pp. 132–139, Nov. 2000.

[32] A.-A. A. Boulogeorgos, P. C. Sofotasios, S. Muhaidat, M. Valkama, and G. K. Karagiannidis, "The effects of RF impairments in vehicle-to-vehicle communications," in *Proc. IEEE 25th Int. Symp. PIMRC PHY*, Hong Kong, Aug. 2015, pp. 840–845.

[33] A.-A. A. Boulogeorgos, P. C. Sofotasios, B. Selim, S. Muhaidat, G. K. Karagiannidis, and M. Valkama, "Effects of RF impairments in communications over cascaded fading channels," *IEEE Trans. Veh. Technol.*, vol. 65, no. 11, pp. 8878–8894, Nov. 2016.

[34] A.-A. A. Boulogeorgos, P. C. Sofotasios, B. Selim, S. Muhaidat, G. K. Karagiannidis, and M. Valkama, "Outage probability under I/Q imbalance and cascaded fading effects," presented at the Int. Conf. Telecommun., Thessaloniki, Greece, May 2016.

[35] M. Mokhtar, A.-A. A. Boulogeorgos, G. K. Karagiannidis, and N. Al-Dhahir, "OFDM opportunistic relaying under joint transmit/receive I/Q imbalance," *IEEE Trans. Commun.*, vol. 62, no. 5, pp. 1458–1468, May 2014.

[36] M. Mokhtar, A.-A. A. Boulogeorgos, G. K. Karagiannidis, and N. Al-Dhahir, "Dual-hop OFDM opportunistic AF relaying under joint transmit/receive I/Q imbalance," in *Proc. IEEE Global Telecommun. Conf.*, Atlanta, GA, USA, Dec. 2013, pp. 4287–4292.

[37] A.-A. A. Boulogeorgos, V. M. Kapinas, R. Schober, and G. K. Karagiannidis, "I/Q-imbalance self-interference coordination," *IEEE Trans. Wireless Commun.*, vol. 15, no. 6, pp. 4157–4170, Jun. 2016.

[38] A.-A. A. Boulogeorgos, D. S. Karas, and G. K. Karagiannidis, "How much does I/Q imbalance affect secrecy capacity?" *IEEE Commun. Lett.*, vol. 20, no. 7, pp. 1305–1308, Jul. 2016.

[39] H. Bany Salameh, M. Krunz, and O. Younis, "Cooperative adaptive spectrum sharing in cognitive radio networks," *IEEE/ACM Trans. Netw.*, vol. 18, no. 4, pp. 1181–1194, Aug. 2010.
[40] H. Bany Salameh and M. El-Attar, "Cooperative OFDM-based virtual clustering scheme for distributed coordination in cognitive radio networks," *IEEE Trans. Veh. Technol.*, vol. 64, no. 8, pp. 3624–3632, Aug. 2015.
[41] A. Papoulis and S. Pillai, *Probability, Random Variables, and Stochastic Processes*, ser. McGraw-Hill series in electrical engineering: Communications and signal processing. Noida, India: Tata McGraw-Hill, 2002.

Alexandros-Apostolos A. Boulogeorgos (S'11) was born in Trikala, Greece. He received the Diploma degree (five years) in electrical and computer engineering from the Aristotle University of Thessaloniki, Thessaloniki, Greece, in 2012. He is currently working toward the Ph.D. degree with the Department of Electrical and Computer Engineering, Aristotle University of Thessaloniki.

His current research interests are in the areas of fading-channel characterization, cooperative communications, cognitive radio, interference management, and hardware-constrained communications.

Haythem A. Bany Salameh (SM'16) received the Ph.D. degree in electrical and computer engineering from The University of Arizona, Tucson, AZ, USA, in 2009.

He is currently an Associate Professor of telecommunication engineering with Yarmouk University (YU), Irbid, Jordan, where he has been the Director of the Queen Rania Center for Jordanian Studies and Community Service since June 2014. From January 2011 to June 2014, he was the Director of the Academic Entrepreneurship Center of Excellence at YU. In the summer of 2008, he was a member of the R&D Long-Term Evolution Development Group at Qualcomm, Inc., San Diego, CA, USA. In summer 2015, he was a Visiting Research Professor with the Telecommunications Systems and Networks Laboratory, Aristotle University of Thessaloniki, Thessaloniki, Greece. His research is in wireless communications technology and computer networking, with emphasis on resource allocation, adaptive control, and distributed protocol design. He was involved in projects related to optical communications and wireless sensor networks.

Dr. Salameh has served on the Technical Program Committee of many international conferences. He has served and continues to serve as a reviewer for many international conferences and journals.

George K. Karagiannidis (M'96–SM'03–F'14) was born in Pythagorion, Samos Island, Greece. He received the University Diploma (five years) and Ph.D. degrees in electrical and computer engineering from the University of Patras, Patras, Greece, in 1987 and 1999, respectively.

From 2000 to 2004, he was a Senior Researcher with the Institute for Space Applications and Remote Sensing, National Observatory of Athens, Athens, Greece. In June 2004, he joined the faculty of Aristotle University of Thessaloniki, Thessaloniki, Greece, where he is currently a Professor with the Department of Electrical and Computer Engineering and the Director of the Digital Telecommunications Systems and Networks Laboratory. He is also currently an Honorary Professor at Southwest Jiaotong University, Chengdu, China. He has authored or coauthored over 400 technical papers published in scientific journals and presented at international conferences. He has also authored the Greek edition of a book on telecommunications systems and has coauthored *Advanced Optical Wireless Communications Systems* (Cambridge, 2012). His research interests are in the broad area of digital communications systems, with emphasis on wireless communications, optical wireless communications, wireless power transfer and applications, molecular communications, communications and robotics, and wireless security.

Dr. Karagiannidis has been involved as a General Chair, a Technical Program Chair, and a member of technical program committees of several IEEE and non-IEEE conferences. He was an Editor of the IEEE TRANSACTIONS ON COMMUNICATIONS, a Senior Editor of the IEEE COMMUNICATIONS LETTERS, an Editor of the EURASIP *Journal of Wireless Communications and Networking*, and, several times, a Guest Editor of the IEEE TRANSACTIONS ON SELECTED AREAS ON COMMUNICATIONS. From 2012 to 2015, he was the Editor-in-Chief of the IEEE COMMUNICATIONS LETTERS. He has been selected as a 2015 Thomson Reuters Highly Cited Researcher.